References

BOKHENKOV, E. L., RODINA, E. M., SHEKA, E. F. & NATKANIEC, I. (1978). *Phys. Status Solidi*, **85**, 331–342.
BROCK, C. P. & DUNITZ, J. D. (1982). *Acta Cryst.* B**38**, 2218–2228.
BROCK, C. P. & DUNITZ, J. D. (1990). *Acta Cryst.* B**46**, 795–806.
CRIADO, A. (1989). *Acta Cryst.* A**45**, 409–415.
CRUICKSHANK, D. W. J. (1956*a*). *Acta Cryst.* **9**, 915–923.
CRUICKSHANK, D. W. J. (1956*b*). *Acta Cryst.* **9**, 1005 1009.
CRUICKSHANK, D. W. J. (1957). *Acta Cryst.* **10**, 504–508.
DORNER, B., BOKHENKOV, E. L., CHAPLOT, S. L., KALUS, J., NATKANIEC, I., PAWLEY, G. S., SCHMELZER, U. & SHEKA, E. F. (1982). *J. Phys. C*, **15**, 2353–2365.
EISENSTEIN, M. (1988). *Int. J. Quantum Chem.* **33**, 127 158.
FILIPPINI, G., GRAMACCIOLI, C. M., SIMONETTA, M. & SUFFRITTI, G. B. (1973). *J. Chem. Phys.* **59**, 5088 5101.
GRAMACCIOLI, C. M. & FILIPPINI, G. (1983). *Acta Cryst.* A**39**, 784 791.
HANSEN, N. K. & COPPENS, P. (1978). *Acta Cryst.* A**34**, 909–921.
HARADA, J. & SAKATA, M. (1974). *Acta Cryst.* A**30**, 77–82.
HIRSHFELD, F. L. (1976). *Acta Cryst.* A**32**, 239–244.
HIRSHFELD, F. L. (1977*a*). *Theor. Chim. Acta*, **44**, 129–138.
HIRSHFELD, F. L. (1977*b*). *Isr. J. Chem.* **16**, 226–229.
HIRSHFELD, F. L. (1991). *Crystallogr. Rev.* In the press.
KITAIGORODSKY, A. (1966). *J. Chim. Phys.* **63**, 6–14.
NATKANIEC, I., BOKHENKOV, E. L., DORNER, B., KALUS, J., MACKENZIE, G. A., PAWLEY, G. S., SCHMELZER, U. & SHEKA, E. F. (1980). *J. Phys. C*, **13**, 4265–4283.
PAWLEY, G. S. (1967). *Phys. Status Solidi*, **20**, 347–360.
PAWLEY, G. S. (1972). *Advances in Structure Research by Diffraction Methods*, Vol. 4, edited by W. HOPPE & R. MASON, pp. 1–64. Oxford: Pergamon Press.
RUYSINK, A. F. J. & VOS, A. (1974). *Acta Cryst.* A**30**, 503–506.
STEWART, R. F. W. (1976). *Acta Cryst.* A**32**, 565–574.
SUZUKI, M., YOKOYAMA, T. & ITO, M. (1968). *Spectrochim. Acta Part A*, **24**, 1091–1107.
TRUEBLOOD, K. N. (1978). *Acta Cryst.* A**34**, 950–954.
VOVELLE, F., CHEDIN, M. P. & DUMAS, G. G. (1978). *Mol. Cryst. Liq. Cryst.* **48**, 261–271.
WILLIAMS, D. E. (1967). *J. Chem. Phys.* **47**, 4680–4684.

Acta Cryst. (1991). B**47**, 797–806

High-Pressure Phases of Cyclohexane-d_{12}*

BY N. B. WILDING, P. D. HATTON† AND G. S. PAWLEY

Department of Physics, University of Edinburgh, Mayfield Road, Edinburgh EH9 3JZ, Scotland

(*Received* 3 *September* 1990; *accepted* 15 *April* 1991)

Abstract

A neutron powder diffraction study has been performed to investigate the high-pressure phases of deuterated cyclohexane. The unit cell and space group of the previously unsolved high-pressure phases III and IV have been determined with the aid of *KOHL* – a version of Kohlbeck & Hörl's *TMO* indexing program [*J. Appl. Cryst.* (1978), **11**, 60–61]. At 5 kbar, 280 K, we find that phase III is orthorhombic with unit-cell parameters $a = 6{\cdot}587\ (3)$, $b = 7{\cdot}844\ (7)$, $c = 5{\cdot}295\ (3)$ Å, $Z = 2$, space group $Pmnn$, $R_I = 4{\cdot}2$, $R_{wp} = 8{\cdot}4\%$. Approximate molecular orientations have also been determined for phase III using a combination of lattice-energy minimization techniques and constrained Rietveld refinement. On decreasing the temperature at 5 kbar, a structural phase transition was observed at 265 K to phase IV, a monoclinic structure with unit-cell parameters $a = 6{\cdot}526\ (4)$, $b = 7{\cdot}597\ (6)$, $c = 5{\cdot}463\ (5)$ Å, $\beta = 97{\cdot}108\ (4)^\circ$ at 250 K, $Z = 2$, space group $P12_1/n1$. This phase, which was observed down to 175 K, is closely related to the orthorhombic phase III but differs greatly from the monoclinic phase II which exists under atmospheric pressure at temperatures below 186·1 K. A further phase transition between phases IV and II was found at 2 kbar, 175 K.

1. Introduction and background

It is a feature of many organic molecular crystals that they exhibit a rich variety of phase structure, both as a function of temperature and pressure. Although the adoption by a molecular crystal of a range of different structures is thought to owe much to the rules of compact packing, this is by no means the sole criterion and further influencing factors such as the directionality of bonding may also play a role (Kitaigorodski, 1971). The lack of a thorough understanding of the processes governing the formation of any given phase means that as yet, it is not possible to predict, *a priori*, which structure a given molecular crystal will adopt for prescribed values of the temperature and pressure. A clear elucidation for a simple molecular system of the adopted structures, together with the conditions under which they are formed is therefore a vital step towards the understanding of the mechanisms governing structural polymorphism. To this end we have chosen to investigate the high-pressure phases of cyclohexane which, whilst being a relatively simple and compact molecule, is also known to exhibit a wealth of phase structure.

* Neutron powder diffraction measurements were carried out at the Institut Laue–Langevin, Grenoble.

† Author to whom correspondence should be addressed.

0108-7681/91/050797-10$03.00

Most of the previous structural studies on cyclohexane have focussed on the ambient-pressure phases, which have been extensively investigated using a variety of techniques including X-ray diffraction, infrared spectroscopy and NMR. At ambient pressure two stable solid phases of cyclohexane are known to exist. Phase I, the plastic phase, lies between 186·1 K and the melting point at 279·82 K. It is cubic [a = 8·61 (2) Å, Z = 4, space group $Fm3m$] and from NMR studies is known to be characterized by a large degree of dynamic molecular disorder, the molecules undergoing rapid reorientations on the lattice sites (Andrew & Eades, 1953). Below 186·1 K an order–disorder transition takes place to an orientationally ordered structure (phase II). Single-crystal X-ray diffraction measurements performed by Kahn, Fourme, André & Renaud (1973) have shown that phase II possesses a monoclinic unit cell [a = 11·23 (2), b = 6·44 (2), c = 8·20 (2) Å, β = 108·83°, Z = 4, space group $C2/c$]. In the same work, a determination of the molecular positions and atomic coordinates also revealed that the molecules are in the 'chair' conformation, but exhibit a slight though significant deviation from D_{3d} symmetry.

In contrast to the ambient-pressure phases, relatively little is known about the structures existing at high pressure and it is only comparatively recently that they have come under scrutiny. Previous high-pressure investigations have been carried out using differential thermal analysis (DTA), vibrational spectroscopy and neutron powder diffraction techniques.

DTA measurements on the hydrogenated system performed by Würflinger (1975) point clearly to the presence of a new structure (phase III) at pressures above 0·25 kbar. The temperature range over which this phase is stable was observed to increase with pressure. Similar DTA work by the same group on the deuterated system also indicated the existence of a further high-pressure structure (phase IV), lying intermediate between phase III and the low-temperature structure (Schulte & Würflinger, 1987). Phase IV is not observed in the hydrogenated system, suggesting that deuteration plays a major role in determining the high-pressure structure. Reproductions of the phase diagrams of Schulte & Würflinger for both C_6H_{12} and C_6D_{12} up to 3 kbar are included in Figs. 1(*a*) and 1(*b*).

Ambient-temperature vibrational spectroscopy measurements on both C_6H_{12} and C_6D_{12} as a function of pressure have recently been reported by Haines & Gilson (1989, 1990). Using Raman and infrared techniques, these workers detected two phase transitions in both molecular systems. In the deuterated system, the first transition occurred at 5·3 kbar with the second appearing at 7·4 kbar. In contrast, for the hydrogenated system, phase transitions were seen at 5·1 and 9·6 kbar. From an analysis of the vibrational modes of both systems, the phase above the first transition (*i.e.* at higher pressure), was found to possess orthorhombic D_{2h} site symmetry. A similar analysis for the upper phase suggested that here the molecules possess monoclinic C_{2h} site symmetry, prompting the conclusion that the upper phase is none other than the monoclinic phase II. No clear findings relating to a transition above 7·4 kbar have been reported by Haines & Gilson, though recent and as yet unpublished Raman measurements at Edinburgh have revealed a room-temperature transition at approximately 12 kbar in the deuterated system (Poon, 1990). Such a transition pressure is consistent with an albeit large linear extrapolation to room temperature of the phase II to phase IV boundary shown to 3 kbar in Fig. 1(*b*).

The DTA results for phase III in both C_6D_{12} and C_6H_{12} can be seen to be consistent with those of the

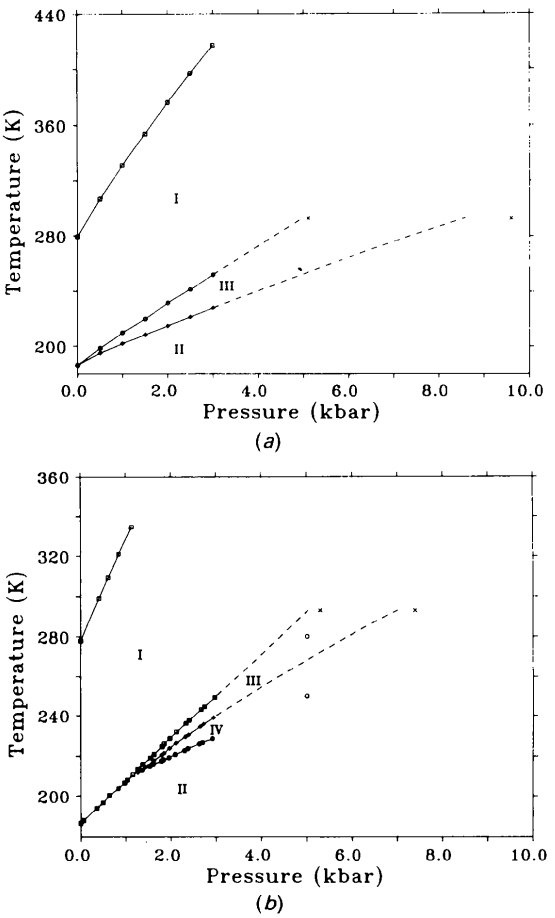

Fig. 1. The phase diagram of Schulte & Würflinger (1987) for (*a*) cyclohexane and (*b*) cyclohexane-d_{12}. The broken lines represent the extrapolation to room temperature of a polynomial fit to the DTA data. The points (×) at 293 K correspond to the boundary of phase III as determined by Haines & Gilson (1989, 1990). The points (○) at 5 kbar, 280 K and 5 kbar, 250 K indicate our own data points for which structural determinations were performed.

vibrational spectroscopy, by means of an extrapolation to 293 K of the phase diagrams of Schulte & Würflinger (1987). Using a polynomial fit based solely on the DTA data, we have projected the phase lines delineating phase III to room temperature (Fig. 1, broken lines). For the hydrogenated system this procedure yields transitions at approximately 5·0 and 8·6 kbar, whilst for the deuterated system we find transitions at 5·1 and 7·0 kbar. Evidently these estimates are in reasonable accord with the values measured by Haines & Gilson. There seems little doubt, therefore, that in both C_6D_{12} and C_6H_{12}, the structure existing at pressures slightly above 5 kbar at 293 K is phase III, as defined in the phase diagrams of Fig. 1.

Neutron powder diffraction studies of C_6D_{12} have been performed very recently by Mayer *et al.* (1990, 1991) for pressures in the range 1 bar to 3·7 kbar and temperatures down to 160 K. This investigation confirmed the presence of the phases observed in the DTA work and showed that the crystal structures of the various phases (I–IV) differ. Moreover, the study revealed that the high-pressure phases can exhibit a surprising degree of metastability, strongly dependent on the thermodynamic history of the sample. Thus, for example, it was found that phase IV (as defined in the phase diagram of Fig. 1*b*) is obtained only if the sample is first cooled to phase II, followed by the application of pressure, and finally by the raising of the temperature. Other thermodynamic paths such as the application of pressure at room temperature followed by cooling, allowed phase IV to be supercooled (relative to Fig. 1*b*) by several tens of degrees. Owing to low instrumental resolution, the quality of the diffraction data from this study was inadequate to allow a determination of the unknown crystal structures of phases III and IV.

Given the lack of a detailed structure determination for either phase III or IV, and the consequent limitations for an understanding of the effect of deuteration on the phase diagram, we have sought to make a determination of the high-pressure structures of the deuterated system. As single-crystal work at high pressure is fraught with difficulties, we have performed a high-resolution neutron powder diffraction study. Due to the typically large number of overlapping reflections seen in a powder profile, access to a large-wavelength neutron source and a high-resolution diffractometer were essential to the feasibility of this study.

2. Experimental and structure determination

All data were collected using the high-resolution D1A neutron diffractometer at the Institut Laue–Langevin (ILL) (Hewat & Bailey, 1976). A large incident neutron wavelength of 2·989 ± 0·001 Å was used and calibrated using a silicon wavelength standard. At this wavelength, a 1% $\lambda/3$ contamination was present in the beam, originating from the germanium monochromator. For high-pressure measurements at low temperatures, a 6 kbar helium pressure cell was employed in conjunction with a standard orange cryostat. The pressure as indicated by the calibration of the pumping apparatus was

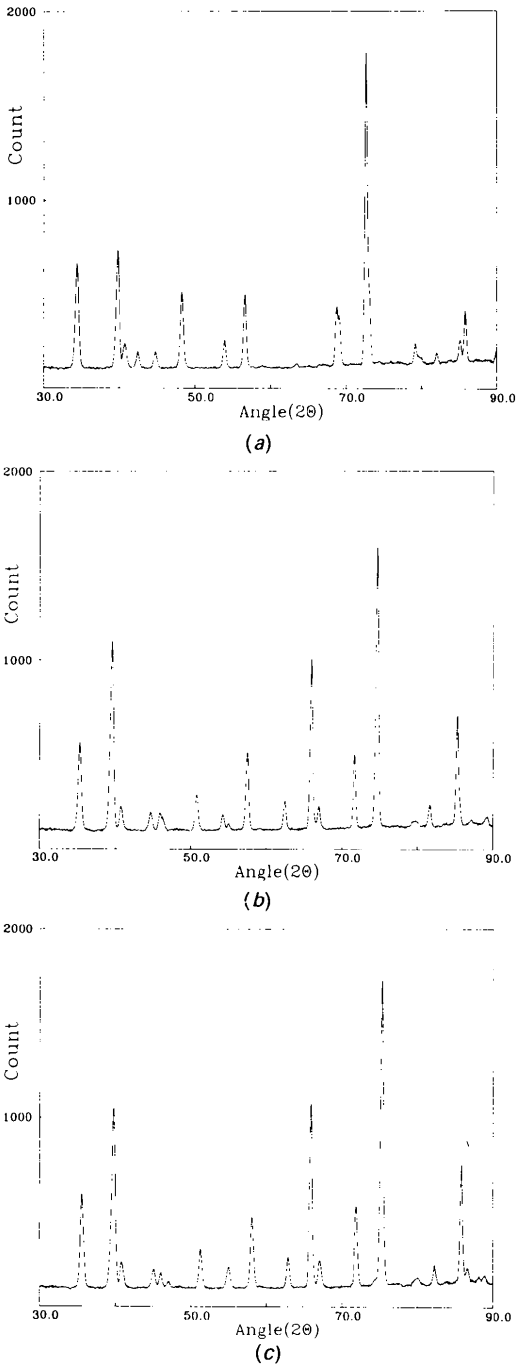

Fig. 2. Profile patterns at 5 kbar for C_6D_{12} at (*a*) 280 K, (*b*) 250 K and (*c*) 175 K.

independently corroborated by a strain-gauge instrument accurate to better than 0·1 kbar.

A commercially available sample of C_6D_{12} with a stated deuterium purity of 99·5% was obtained from the Aldrich Chemical Company. The sample was introduced in liquid form to the sample holder, a 12 mm diameter vanadium can. In order to ensure homogeneity of the powder, the sample can was packed with silica wool prior to the introduction of the sample. In this way, no single crystals of significant size could be formed on cooling. The effect of the silica wool on the powder patterns is known to be negligible, adding uniformly to the background (Baharie & Pawley, 1977).

The aluminium housing of the pressure cell gave rise to a main diffraction peak (200), centred at 94° of 2θ. The corresponding $\lambda/3$ contamination was identified at 28·5°, with further peaks at 40·8 and 79·5°. Those reflections lying in the immediate vicinity of these reflections were excluded from the set used for the cell-indexing procedure. At a pressure of 5 kbar, scans were collected at temperatures of 280, 250 and 175 K. Whilst maintaining the temperature constant at 175 K, the pressure was then reduced in successive steps to 3, 2, 1 kbar and finally to 1 bar. The constant-pressure powder patterns are presented in Fig. 2, while those at constant temperature are given in Fig. 3.* In the interests of clarity these patterns have been truncated to show only the portions between 30 and 90° of 2θ.

2.1. *Phase* III: *the orthorhombic phase*

Initially a short run was performed at 5 kbar, 300 K, yielding a rather featureless powder pattern of few peaks, consistent with the high symmetry of the cubic structure and dynamic orientational disorder. The temperature was then reduced to 280 K whereupon it became evident that a phase transition had occurred. A data set of substantial duration (12 h) was then collected at this temperature yielding

* The numbered intensities of each measured point on the profiles have been deposited with the British Library Document Supply Centre as Supplementary Publication No. SUP 54206 (49 pp.). Copies may be obtained through The Technical Editor, International Union of Crystallography, 5 Abbey Square, Chester CH1 2HU, England.

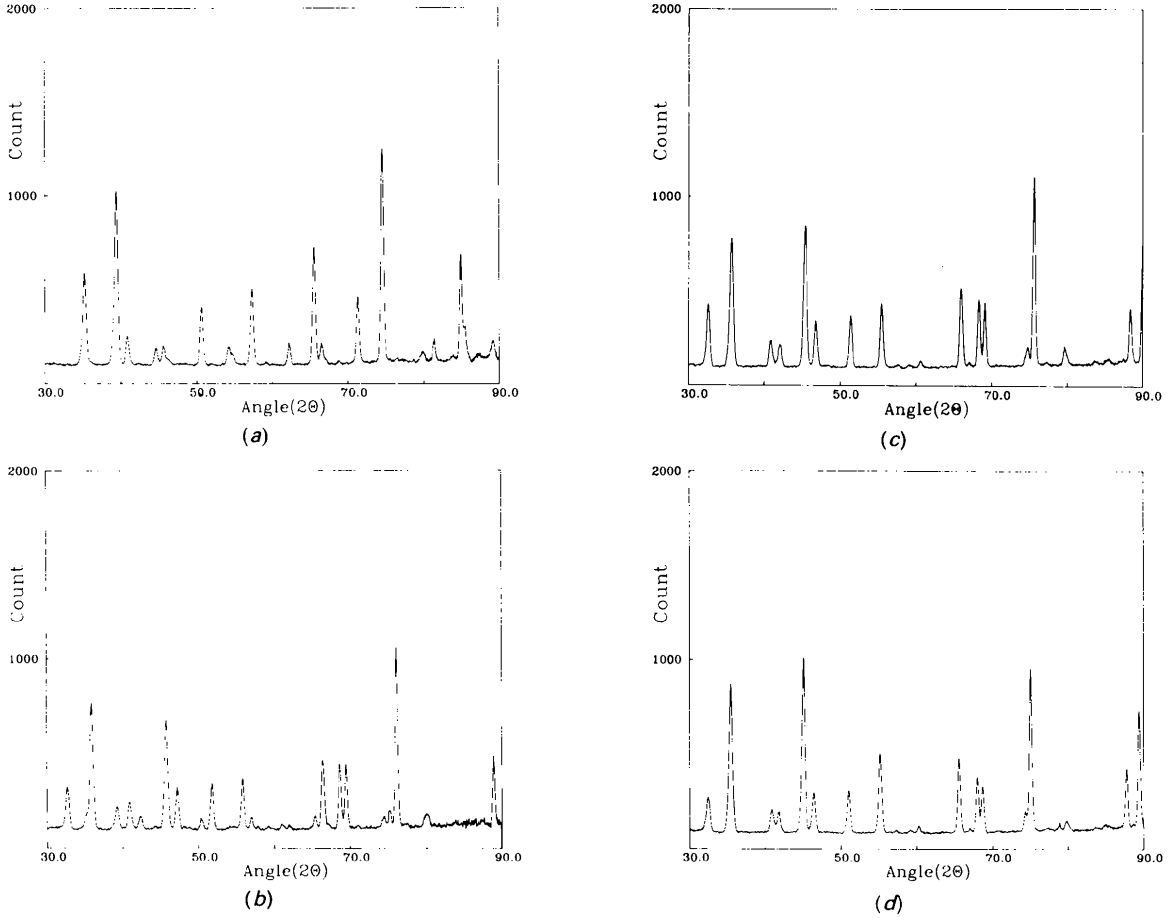

Fig. 3. Profile patterns at 175 K for C_6D_{12} at (*a*) 3 kbar, (*b*) 2 kbar, (*c*) 1 kbar and (*d*) 1 bar.

Table 1. *Observed and calculated reflections of cyclohexane-d_{12} at 5 kbar, 280 K in the space group Pmnn*

The calculated reflections were generated using the refined cell parameters given in Table 3. Those reflections which may not have been resolved are marked by an asterix (*). The 301 reflection has not been assigned an intensity as it lies very close to the 200 aluminium line. 2θ(zero) is 2θ(obs) + 0·051 .

h	k	l	Count	2θ(zero) ( )	2θ(calc) ( )	$\Delta(2\theta)$ ( )
1	1	0	670	34·478	34·476	0·002
0	1	1	737	39·826	39·828	0·002
1	0	1	198	42·462	42·473	−0·011
0	2	0	196	44·762	44·809	−0·047
1	1	1	519	48·320	48·320	0·000
2	0	0	270	53·975	53·985	0·010
0	2	1	504	56·620	56·629	0·009
1	2	1	137	63·520	63·445	0·075
0	0	2	441	68·810	68·752	0·058
2	1	1	392	69·098	69·148	−0·050
2	2	0	1784	72·710	72·695	0·015
0	1	2		*	73·10	
1	3	0			75·87	
1	1	2		*	79·18	
0	3	1	249	79·236	79·229	0·007
2	2	1	200	82·083	82·065	0·018
1	3	1	263	85·188	85·188	0·000
0	2	2	413	85·849	85·879	0·030
3	1	0	207	89·991	89·980	0·011
1	2	2			91·73	
2	0	2	312	92·855	92·843	0·012
3	0	1		94·894	94·910	0·016
2	1	2	248	97·013	97·021	0·008
3	1	1	885	99·134	99·152	0·018
0	4	0		*	99·28	
2	3	1			102·96	
0	3	2	533	106·900	106·936	0·036
0	4	1	194	108·769	108·757	0·012
2	2	2	206	109·890	109·885	0·005
3	2	1	332	112·151	112·145	0·006
1	3	2			113·17	
1	4	1			115·07	
0	1	3	314	120·459	120·437	0·022
1	0	3	317	122·463	122·479	0·016
2	4	0			124·99	
3	3	0	1081	125·428	125·452	−0·024
1	1	3	247	127·593	127·550	0·043
3	1	2			129·53	
4	0	0	289	130·311	130·340	0·029

data in the 2θ range 10–130° for a 2θ step size of 0·05°. A portion of the resulting profile is presented in Fig. 2(*a*). In the light of the DTA and spectroscopic results discussed above, we assumed the 280 K pattern corresponded to phase III, and proceeded to attempt to determine its structure.

Automatic indexing of the 280 K pattern was carried out using *KOHL*, an adaptation (Shirley, 1978) of the *TMO* program of Kohlbeck & Hörl (1978), which uses semi-exhaustive, index-trial methods for the *ab initio* determination of unit-cell parameters from powder patterns of single solid phases, for all symmetries down to triclinic. In common with most indexing programs, *KOHL* requires 20 preferably low-angle reflections for its operation. A figure of merit is attached to each solution and this assessment criterion and its reliability have been discussed by de Wolff (1968).

Table 1 includes a list of all the observed sample reflections and their intensities for the 280 K pattern as a function of 2θ. Using as input the 20 lowest-angle reflections of reasonable intensity, the program produced a number of candidate solutions only one of which successfully indexed all 20 lines. The second and subsequent candidate lattices matched 15 or fewer lines and were clearly inconsistent with many of the observed reflections. They were thus duly discarded as incorrect. The accepted solution, to which the program assigned a high figure of merit (25·3), gave an orthorhombic unit cell with parameters $a = 6{\cdot}580$, $b = 7{\cdot}839$, $c = 5{\cdot}289$ and a primitive lattice. Clearly the volume for this unit cell ($V = 273$ Å^3) is approximately half that of the cell of phase II at ambient pressure ($V = 561$ Å^3). Accordingly we postulate that $Z = 2$ for phase III.

With the unit cell from *KOHL*, it was possible, by noting the systematic absences in the reflection list, to deduce the following reflection conditions: $h0l$: $h + l = 2n$, $hk0$: $h + k = 2n$, $h00$: $h = 2n$, $0k0$: $k = 2n$, $00l$: $l = 2n$. These reflections are consistent with either the centrosymmetric space group *Pmnn* or noncentrosymmetric *P2nn* (Nos. 58 and 34 respectively). For expediency, we shall assume the high-symmetry space group *Pmnn* and justify this choice *a postiori*.

The symmetry operators of the space group *Pmnn* dictate that, given two compact molecules in the unit cell, the centre of one molecule must coincide with a lattice site at the cell corner whilst the other must occupy the body centre. The space group also has a centre of symmetry and a mirror plane at $x = 0$, which place restrictions on the atomic positions. The deduced lattice parameters were refined in conjunction with the profile data, using the *ALLHKL* program of Pawley (1981). Refined values for the cell parameters are to be found in Table 3. These parameters were used to generate the calculated reflection angles, also listed in Table 1.

The approximate molecular orientation for phase III was determined using a combination of lattice-energy minimization and constrained Rietveld refinement as follows. Initially, an idealized rigid 'chair-shaped' cyclohexane molecule was assumed having tetrahedral bond angles and D_{3d} symmetry. The coordinates of this molecule, which are identical to those used for the molecular-dynamics simulations of Trew, Pawley & Cairns-Smith (1990), are given in Table 4, and the molecule is represented pictorially in Fig. 4. By virtue of the mirror plane at $x = 0$, the one twofold rotation axis of the molecule is preserved and is constrained to coincide with the x axis, permitting the rigid molecule only a single degree of freedom, namely a rotation about the x axis.

Using the deduced unit-cell parameters and idealized molecule, energy minimization was performed for a cluster of 109 rigid deuterated molecules. The potential employed was of the Buckingham form with the parameters of Williams (1967). Monitoring

Table 2. *Observed and calculated reflections of cyclohexane-d_{12} at 5 kbar, 250 K in the space group $P12_1/n1$*

The calculated reflections were generated using the refined cell parameters given in Table 3. The 122 and $\bar{3}11$ reflections have not been assigned an intensity as they lie very close to the 200 aluminium line. Those reflections which may not have been resolved are marked by an asterix (*). The apparently unobserved reflections $\bar{1}31$ and 131 are coincident with their neighbours and are visible in the 5 kbar, 175 K pattern. 2θ(zero) is 2θ(obs) + 0·004°.

h	k	l	Count	2θ(zero) (°)	2θ(calc) (°)	$\Delta(2\theta)$ (°)
1	1	0	566	35·318	35·305	0·013
−1	0	1		*	39·38	
0	1	1	1100	39·545	39·595	−0·050
1	0	1	202	44·720	44·768	−0·048
−1	1	1	205	45·908	45·929	−0·021
0	2	0	172	46·273	46·338	−0·065
1	1	1	291	50·796	50·761	0·035
1	2	0	190	54·304	54·276	0·028
2	0	0	141	55·022	54·975	0·047
0	2	1	511	57·466	57·427	0·039
2	1	0			60·23	
−1	2	1	252	62·440	62·397	0·043
−2	1	1	1016	65·972	65·953	0·019
1	2	1			66·39	
0	0	2	235	66·978	66·929	0·049
0	1	2	493	71·665	71·671	−0·006
2	1	1			73·65	
−1	1	2		*	74·28	
2	2	0	1609	74·626	74·672	−0·046
1	3	0			78·64	
−2	2	1			79·90	
0	3	1		*	81·29	
1	1	2	242	81·641	81·664	−0·023
−2	0	2			84·73	
0	2	2	363	85·288	85·280	0·008
−1	3	1		*	85·62	
2	2	1	164	87·196	87·17	0·026
−1	2	2			87·78	
−2	1	2	180	89·218	89·176	0·042
1	3	1		*	89·230	
−3	0	1			90·92	
3	1	0			92·06	
1	2	2		95·001	95·013	−0·012
−3	1	1		95·354	95·371	−0·017
2	3	0	316	97·075	97·045	0·030
2	0	2			99·21	
3	0	1	231	101·855	101·839	0·016
−2	2	2	522	102·522	102·581	−0·059
2	1	2	308	103·719	103·743	−0·024
0	4	0		*	103·79	
3	2	0	144	105·536	105·560	−0·024
3	1	1	154	106·433	106·413	0·020
0	3	2	367	107·721	107·741	−0·020
−3	2	1	414	108·986	109·014	−0·028
2	3	1	138	109·785	109·732	0·053
1	4	0	165	110·205	110·176	0·029
1	3	2		*	110·38	
−1	0	3	208	112·367	112·353	0·014
0	4	1			112·98	
0	1	3	178	116·468	116·461	0·007

the energy as a function of angle for a rotation of 90° about the x axis yielded a global energy minimum when the vector from the origin to the C3 atom is inclined at 38·48° to the y axis.

The molecular orientation obtained from energy minimization was used as the starting point for a Rietveld refinement of the powder profile. This was carried out using the *PROFIL* neutron powder refinement program available at ILL (Cockcroft, 1989). Initially eight parameters were refined (cell parameters, scale, zero error and U, V, W) with no adjustment of atomic coordinates. The background was treated by a polynomial fit to 150 visually

Table 3. *Lattice parameters of cyclohexane-d_{12} at 5 kbar for T = 280, 250 and 175 K*

Parameter	280 K	250 K	175 K
a (Å)	6·587 (3)	6·526 (4)	6·518 (5)
b (Å)	7·844 (7)	7·597 (6)	7·496 (7)
c (Å)	5·295 (3)	5·463 (5)	5·460 (4)
β (°)	90	97·108 (4)	97·725 (3)
Volume (Å^3)	273·64 (4)	268·71 (3)	264·42 (4)

Table 4. *Atomic coordinates (Å) of the idealized molecule used for energy minimization calculations*

Only half the atoms of the molecule are given, the remainder follow from an inversion through the origin

Parameter	x	y	z
C1	1·2664	0·7311	0·2585
C2	1·2664	0·7311	0·2585
C3	0·0000	−1·4623	−0·2585
D1	1·2664	0·7311	1·2315
D2	1·2664	−0·7311	1·2315
D3	0·0000	−1·4623	1·2315
D4	2·0608	1·1898	0·0658
D5	2·0608	−1·1898	0·0658
D6	0·0000	−2·3796	0·0658

estimated points and a pseudo-Voigt peak shape was employed to model the observed peaks. Isotropic thermal parameters were not refined and were set to 5·53 for deuterium and 1·11 for carbon atoms. The refinement converged quickly with a final intensity R factor of 8%, where we used $R_I \equiv \sum_i |Y_i^{obs} - Y_i^{calc}| / \sum_i Y_i^{calc}$. Chemical or 'slack' constraints were then placed on the bond lengths and angles so that they should favour the geometry of the idealized molecule. This brought the number of refinable parameters to 19. The size of the maximum permitted deviation of the bond parameters from the idealized structure was limited (somewhat arbitrarily) to be consistent with the deviation from the ideal geometry observed by Kahn *et al.* (1973) for phase II. Of course, the constraints imposed by the space-group symmetry were not relaxed.

Allowing refinement under these constraints, the intensity R factor improved markedly to 4%. The

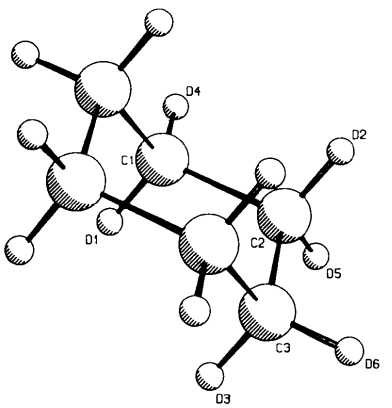

Fig. 4. The ideal cyclohexane molecule in the 'chair' conformation. The molecule has D_{3d} symmetry and tetrahedral bond angles.

refined profile is presented in Fig. 5 with the corresponding atomic coordinates, principal bond parameters and refinement parameters appearing in Tables 5, 6 and 7 respectively. Notwithstanding the relatively poor resolution on short-length scales ($\leq 1{\cdot}5$ Å) resulting from the large wavelength, it is apparent from the bond parameters that the molecule exhibits a significant deviation from D_{3d} symmetry and tetrahedral bonding. The size of this deviation is, however, not inconsistent with that observed by Kahn *et al.* (1973) for phase II. A carbon skeletal representation of the refined molecular arrangement relative to the unit cell is shown in Fig. 6. The success of the refinement suggests that the centrosymmetric space group is indeed the appropriate choice for this structure.

2.2. *Phase* IV: *the monoclinic phase*

A number of short data sets were collected at 5 kbar between 280 and 260 K in 5 K steps, in order

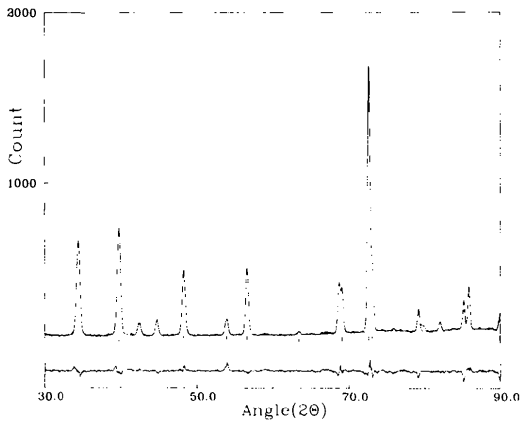

Fig. 5. A difference plot of the refined profile of phase III at 5 kbar, 280 K.

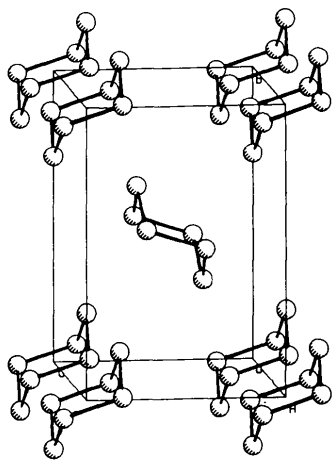

Fig. 6. The refined structure of phase III relative to the orthorhombic unit cell. Note the 'herringbone' molecular stacking common to many organic molecular crystals.

Table 5. *Refined atomic coordinates of cyclohexane-d_{12} at* 5 kbar, 280 K

Parameter	x	y	z
C1	0·192 (2)	0·033 (1)	−0·148 (1)
C3	0·0000	−0·163 (2)	0·166 (2)
D1	0·192 (2)	−0·066 (2)	−0·273 (2)
D3	0·0000	−0·254 (3)	0·046 (3)
D4	0·313 (3)	0·116 (2)	−0·142 (2)
D6	0·00000	−0·201 (3)	0·360 (3)

Table 6. *Independent bond lengths* (Å) *and principal bond angles* (°) *obtained from the refinement of phase* III *at* 5 kbar, 280 K

C2—C3	1·63 (7)	C3—D3	0·96 (2)
C1—C2	1·65 (6)	C3—D6	1·07 (2)
C1—D1	1·02 (1)	C1—D4	1·03 (1)
C1—C2—C3	104·7 (5)	C2—C3—C2′	102·0 (9)

Symmetry code: (′) $-x, y, z$.

Table 7. *Values of the instrumental parameters and R factors for the refinement of the phase* III *powder pattern at* 5 kbar, 280 K

Refined parameters	19
u ( )	0·34
v ( )	0·69
w ( )	0·46
Scale factor	0·0433 (2)
Zero angle ( )	−0·050 (3)
Asymmetry parameter	0·15
2θ refinement range ( )	20–113
2θ step size ( )	0·05
Observed data points	1859
R_I (%)	4·2
R_{wp} (%)	8·4

to establish closely the location of any further transition. At 265 K a clear change in the powder profile was observed, heralding the onset of a new structure. Another short data set at 260 K revealed a pure phase, showing the 265 K profile to be a mixture of the upper and lower phases. The temperature was subsequently reduced further to 250 K to ensure that the sample was fully in the lower phase at that temperature, and a high-quality data set was collected over a period of some 8 h, yielding data in the 2θ range 10–117°. Again a 2θ step size of 0·05° was used. The associated pattern is shown in Fig. 2(*b*).

The indexing procedure described above for phase III was repeated with the 250 K data, the peak positions of the lowest angle reflections (of reasonable intensity) being input to the *KOHL* program. Again this program offered a number of solutions. The 'best', indexing all 20 reflections with a figure of merit of 20·4, was a primitive monoclinic cell with parameters $a = 6{\cdot}523$, $b = 7{\cdot}585$, $c = 5{\cdot}457$ Å, $\beta = 97{\cdot}127°$. The next best solution, with a figure of merit of just 9·3, failed to index some of the reflections and was rejected. A comparison of the above cell with that derived for phase III shows clearly that they are closely related, the transition being affected by a simple tilting of the c axis of the orthorhombic structure concomitant with a small reduction in unit-

cell volume. In view of the previously mentioned DTA and neutron-scattering results, we shall assume the structure at 5 kbar, 250 K to be phase IV.

All the observed sample reflections and their intensities for the 5 kbar, 250 K pattern are included in Table 2. From a consideration of the systematic absences from this reflection list, it transpires that the structure satisfies the following reflection conditions:* $h0l$: $h + l = 2n$, $h00$: $h = 2n$, $0k0$: $k = 2n$, $00l$: $l = 2n$. These reflection conditions are compatible only with the space group $P12_1/n1$ (a setting of $P2_1/c$, b axis unique, cell choice 2, No. 14). Significantly, this space group is a maximal nonisomorphic subgroup of the space group *Pmnn* for the phase III structure, corresponding to the removal of half the symmetry elements in the transition from the orthorhombic to the monoclinic structure. This independent deduction therefore lends weight to the validity of our findings for both structures. In particular the noncentrosymmetric orthorhombic space group *P2nn* is not compatible with the transition to the $P2_1/c$ structure. We note further that the vast majority of organic homomolecular crystals are centrosymmetric and fall into the space group $P2_1/c$ (Belsky & Zorkii, 1977).

The pattern at 5 kbar, 175 K, Fig. 2(*c*), was also subjected to the indexing procedure yielding a 'best' cell of $a = 6{\cdot}511$, $b = 7{\cdot}485$, $c = 5{\cdot}463$ Å, $\beta = 97{\cdot}733°$, with a figure of merit of 25·5. Evidently the structure at this temperature is still essentially the same as that observed at 250 K although the temperature is considerably below that where one would expect to find phase IV according to the phase diagram of Schulte & Würflinger (Fig. 1*b*). No evidence of a phase transformation to phase II was observed at 5 kbar, 175 K even though the sample was maintained under these conditions for a period in excess of 12 h. Clearly this finding is in accord with that of Mayer *et al.* (1991) who observed that the temperature range of stability of phase IV is increased considerably on cooling from phase III compared to heating from phase II.

Both the 250 and the 175 K cell solutions were refined using the *ALLHKL* program, yielding the lattice parameters presented in Table 3. Differences between the profiles of Figs. 2(*b*) and 2(*c*) may be traced to the small difference in the lattice parameters between the two temperatures. The somewhat larger figure of merit of the 175 K indexing compared to that at 250 K arises from the splitting of accidently coincident low-angle peaks which separately receive greater weight in the figure of merit calculation. Those peaks not observed at 250 K (and therefore absent from Table 1) which are apparent in the 175 K data, are the $(\bar{1}31)$ and (131) reflections. It is instructive to try to gauge the angular resolution of the diffraction profile from those close-lying peaks [*e.g.* the (002) and the (221) reflections in Table 1 and Fig. 2*a*] which are only just resolved. From the data it appears that the angular resolution is approximately 0·4°. Thus a number of the reflections apparently absent from Tables 1 and 2 may just not have been resolved. In these cases the table entry for a reflection is marked with an asterix.

In a manner similar to that described for phase III, we have performed energy-minimization calculations for the phase IV structure in an attempt to locate a molecular orientation sufficiently close to the real configuration to permit Rietveld refinement of our powder data. Again the molecular coordinates of Table 4 were used, suitably transformed into the monoclinic basis. However, the task of locating the energy minimum was complicated considerably by the lack in the monoclinic structure of the mirror plane existing in the orthorhombic phase. Consequently, no orientational constraints are imposed on the molecule which thus possesses three degrees of orientational freedom. For a rather compact, spherical molecule such as cyclohexane it is to be expected that a number of spurious local minima exist in the potential energy surface. Indeed this was found to be the case, necessitating an exhaustive search of trial starting orientations, until one lying within the basin of attraction for the global energy minimum was eventually found. A stereoscopic carbon skeletal representation of the molecules in the orientation of minimum energy is given in Fig. 7.

The minimum-energy molecular orientation in phase IV is clearly related to that of phase III. The main qualitative difference appears to be a rotation of the molecular orientation in the same sense as the monoclinic tilt. This 'solution' was used as the starting point for a constrained Rietveld refinement of the powder profiles in which the bonding parameters were again constrained to favour the idealized mol-

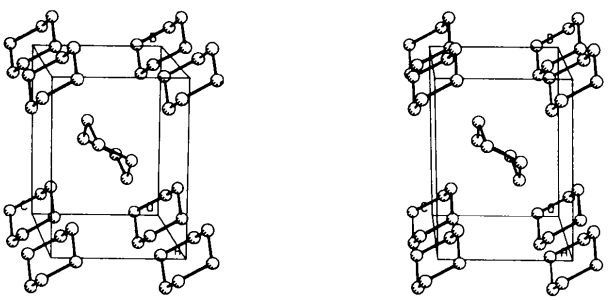

Fig. 7. The minimum potential energy structure for phase IV, obtained using the molecular geometry of Trew *et al.* (1990) combined with the potential parameters of Williams (1967).

* Author's note: in addition to the absence of the 010 and 030 reflections apparent from Table 2, the 050 reflection is also absent from patterns we have collected very recently under the same conditions of temperature and pressure but using a shorter wavelength of 1·59 Å.

ecule. Unfortunately, the best intensity R factor which we could obtain by this process was 18% (for 1959 data points and 35 refined parameters), significantly inferior to that obtained in the orthorhombic phase. We defer discussion of possible reasons for this to the final section.

2.3. *Transition to phase* II

Figs. 3(*a*) to 3(*d*) show the result of decreasing the pressure from 5 kbar at a constant temperature of 175 K. At 3 kbar, Fig. 3(*a*), the structure is evidently still that of phase IV observed at 5 kbar. However at 2 kbar, Fig. 3(*b*), a dramatic change occurs in the powder pattern. By comparing the 1 kbar pattern of Fig. 3(*c*) with that at 3 kbar it is evident that the 2 kbar pattern simply comprises a mixture of the upper and lower pattern, implying phase coexistence. The actual transition pressure is clearly, therefore, very close to 2 kbar. Moreover, the observation of phase coexistence suggests that this transition has first-order character.

The 1 kbar and atmospheric pressure patterns (Figs. 3*c* and 3*d* respectively) correspond to the known structure of phase II as determined by Kahn *et al.* for C_6H_{12}. We have, however, independently indexed the latter profile by way of a test of our indexing procedure. For this pattern, the *KOHL* program yielded a best solution (figure of merit 25·4) with lattice parameters $a = 11{\cdot}28$, $b = 6{\cdot}43$, $c = 8{\cdot}24$ Å, $\beta = 108{\cdot}84°$ and a centred cell, in excellent agreement with the results of Kahn *et al.*

3. Discussion and concluding remarks

The orthorhombic structure of phase III is clearly consistent with the spectroscopic deduction of D_{2h} site symmetry by Haines & Gilson (1989). Their finding of C_{2h} symmetry for the room-temperature structure existing above 7·4 kbar in C_6D_{12} could, however, correspond either to phase II or to phase IV as both possess this site symmetry. Extrapolations of the phase diagram of Schulte & Würflinger (Fig. 1*b*) suggest that phase IV is the best candidate for this phase. Indeed, the recently discovered 12 kbar transition at room temperature, Poon (1990), also appears to be consistent with an extrapolation to room temperature of the phase IV to phase II boundary.

The failure to obtain a satisfactory Rietveld refinement for phase IV may be partially traced to the fact that energy minimization is less powerful when trying to orient 'globular' molecules having unconstrained orientational freedom. Accentuating the problems for accurate Rietveld refinement is the low information content of the data. The need for a large wavelength for indexing purposes unfortunately gives a paucity of Bragg reflections. With as few as 30 distinct peaks in our data, the deviation from the true solution over which the refinement will successfully converge is not great, even with a constrained refinement. This problem is potentially aggravated if the refinement is sensitive to deviations of the molecular geometry from the ideal symmetry, as is seen in the present work for phase III and by Kahn *et al.* (1973) for phase II. It is, therefore, not altogether surprising that a satisfactory determination of the molecular parameters for phase IV was not forthcoming. Nevertheless, we do reserve a greater measure of confidence for our results pertaining to the orthorhombic phase III. Here the molecule is tightly constrained by the space-group symmetry, and we believe that the deduced molecular orientation lies very close to the correct solution.

In summary, we have successfully determined the unit cell and space group for two hitherto unsolved high-pressure phases of deuterated cyclohexane. Approximate atomic coordinates have also been deduced for one of these structures, the orthorhombic phase III. In future neutron powder and Raman spectroscopy work already scheduled, we aim to explore further the high-pressure and low-temperature phases of cyclohexane with a view to extracting the atomic coordinates for phase IV and investigating the nature of the metastability of phase IV with respect to phase II. In order to ameliorate some of the difficulties encountered in the present work, further neutron studies will employ a wavelength of 1·6 Å, thereby permitting a greater number of reflections to be collected.

We would like to express our thanks to Dr A. W. Hewat and Mr John Davies of the Institut Laue–Langevin for their expert assistance during the experiment. Helpful correspondence is also acknowledged with Dr D. Gilson, Dr S. Urban and the referee. One of us (NBW) acknowledges receipt of a Science Faculty scholarship from the University of Edinburgh. This work was funded in part by the Science and Engineering Research Council through research grants and access to the neutron beam facilities at the ILL.

References

ANDREW, E. R. & EADES, R. G. (1953). *Proc. R. Soc. London Ser. A*, **216**, 398–412.
BAHARIE, E. & PAWLEY, G. S. (1977). *J. Appl. Cryst.* **10**, 465–467.
BELSKY, V. K. & ZORKII, P. M. (1977). *Acta Cryst.* A**33**, 1004–1006.
COCKCROFT, J. K. (1989). *PROFIL* program. ILL, Grenoble, France.
HAINES, J. & GILSON, D. F. R. (1989). *J. Phys. Chem.* **93**, 7920–7925.
HAINES, J. & GILSON, D. F. R. (1990). *J. Phys. Chem.* **94**, 4712–4716.

HEWAT, A. W. & BAILEY, I. (1976). *Nucl. Instrum. Methods*, **137**, 463.
KAHN, R., FOURME, R., ANDRÉ, D. & RENAUD, M. (1973). *Acta Cryst.* **B29**, 131–138.
KITAIGORODSKI, A. I. (1971). *Molekularnyje Kristaly*. Moscow: Izd. Nauka.
KOHLBECK, F. & HÖRL, E. M. (1978). *J. Appl. Cryst.* **11**, 60–61.
MAYER, J., CHRUSCIEL, J., HABRYLO, S., HOLDERNA, K., NATKANIEC, I., HARTMANN, M., WÜRFLINGER, A., URBAN, S. & ZAJAC, W. (1990). *High Press. Res.* **4**, 460–462.
MAYER, J., CHRUSCIEL, J., HABRYLO, S., HOLDERNA, K., NATKANIEC, I., HARTMANN, M., WÜRFLINGER, A., URBAN, S. & ZAJAC, W. (1991). *Phys. Status Solidi*. Submitted.
PAWLEY, G. S. (1981). *J. Appl. Cryst.* **14**, 357–361.
POON, W. C.-K. (1990). Private communication.
SCHULTE, L. & WÜRFLINGER, A. (1987). *J. Chem. Thermodyn.* **19**, 363–368.
SHIRLEY, R. (1978). *Crystallographic Computing*, edited by H. SCHENK, R. OLTHOF-HAZEKAMP, H. VAN KONINGSVELD & G. C. BASSI, pp. 221–234. Delft Univ. Press.
TREW, A. S., PAWLEY, G. S. & CAIRNS-SMITH, A. (1990). *Acta Cryst.* A**46**, 979–988.
WILLIAMS, D. E. (1967). *J. Chem. Phys.* **47**, 4680–4684.
WOLFF, P. M. DE (1968). *J. Appl. Cryst.* **1**, 108–113.
WÜRFLINGER, A. (1975). *Ber. Bunsenges. Phys. Chem.* **79**, 1195–1201.

Acta Cryst. (1991). B**47**, 806–813

Structural Study of Aldose Reductase Inhibitors. Ten Oxazolecarbamate Derivatives

BY TOSHIMASA ISHIDA, YASUKO IN, CHIAKI TANAKA AND MASATOSHI INOUE

Osaka University of Pharmaceutical Sciences, 2-10-65 *Kawai, Matsubara, Osaka* 580, *Japan*

(*Received* 11 *March* 1991; *accepted* 7 *May* 1991)

Abstract

(1) Benzyl 4-isopropyl-5-phenyl-2-oxazolecarbamate, $C_{20}H_{20}N_2O_3$, $M_r = 336{\cdot}39$, $P\bar{1}$, $a = 19{\cdot}469\ (7)$, $b = 11{\cdot}270\ (3)$, $c = 8{\cdot}667\ (3)$ Å, $\alpha = 95{\cdot}48\ (3)$, $\beta = 99{\cdot}61\ (3)$, $\gamma = 104{\cdot}96\ (3)^\circ$, $V = 1792\ (1)$ Å^3, $Z = 4$, $D_m = 1{\cdot}266\ (2)$, $D_x = 1{\cdot}247$ g cm^{-3}, λ(Cu $K\alpha$) = 1·5418 Å, $\mu = 6{\cdot}49$ cm^{-1}, $F(000) = 712$, $T = 288$ K, $R = 0{\cdot}048$ for 5244 reflections. (2) Benzyl 4-ethyl-5-phenyl-2-oxazolecarbamate, $C_{19}H_{18}N_2O_3$, $M_r = 322{\cdot}37$, $P2_1/n$, $a = 9{\cdot}131\ (7)$, $b = 18{\cdot}81\ (1)$, $c = 9{\cdot}680\ (8)$ Å, $\beta = 101{\cdot}07\ (3)^\circ$, $V = 1631\ (2)$ Å^3, $Z = 4$, $D_m = 1{\cdot}310\ (2)$, $D_x = 1{\cdot}313$ g cm^{-3}, λ(Cu $K\alpha$) = 1·5418 Å, $\mu = 6{\cdot}92$ cm^{-1}, $F(000) = 680$, $T = 288$ K, $R = 0{\cdot}063$ for 2535 reflections. (3) Benzyl 4-methyl-5-phenyl-2-oxazolecarbamate, $C_{18}H_{16}N_2O_3$, $M_r = 308{\cdot}34$, $P2_1/n$, $a = 9{\cdot}210\ (7)$, $b = 8{\cdot}785\ (6)$, $c = 19{\cdot}800\ (9)$ Å, $\beta = 99{\cdot}60\ (3)^\circ$, $V = 1580\ (2)$ Å^3, $Z = 4$, $D_m = 1{\cdot}299\ (3)$, $D_x = 1{\cdot}300$ g cm^{-3}, λ(Cu $K\alpha$) = 1·5418 Å, $\mu = 6{\cdot}93$ cm^{-1}, $F(000) = 648$, $T = 288$ K, $R = 0{\cdot}057$ for 2190 reflections. (4) Benzyl 5-phenyl-2-oxazolecarbamate, $C_{17}H_{14}N_2O_3$, $M_r = 294{\cdot}31$, $P2_1/c$, $a = 6{\cdot}928\ (1)$, $b = 17{\cdot}255\ (6)$, $c = 25{\cdot}406\ (9)$ Å, $\beta = 92{\cdot}90\ (4)^\circ$, $V = 3033\ (2)$ Å^3, $Z = 8$, $D_m = 1{\cdot}270\ (2)$, $D_x = 1{\cdot}289$ g cm^{-3}, λ(Cu $K\alpha$) = 1·5418 Å, $\mu = 6{\cdot}99$ cm^{-1}, $F(000) = 1232$, $T = 288$ K, $R = 0{\cdot}055$ for 3318 reflections. (5) Benzyl 5-*tert*-butyl-2-oxazolecarbamate, $C_{15}H_{18}N_2O_3$, $M_r = 274{\cdot}33$, $C2/c$, $a = 19{\cdot}38\ (2)$, $b = 6{\cdot}458\ (4)$, $c = 26{\cdot}22\ (3)$ Å, $\beta = 109{\cdot}81\ (9)^\circ$, $V = 3087\ (5)$ Å^3, $Z = 8$, $D_m = 1{\cdot}201\ (5)$, $D_x = 1{\cdot}180$ g cm^{-3}, λ(Cu $K\alpha$) = 1·5418 Å, $\mu = 6{\cdot}44$ cm^{-1}, $F(000) = 1168$, $T = 288$ K, $R = 0{\cdot}049$ for 2169 reflections. (6) Benzyl 4,5-dimethyl-2-oxazolecarbamate, $C_{13}H_{14}N_2O_3$, $M_r = 246{\cdot}27$, $P\bar{1}$, $a = 11{\cdot}086\ (4)$, $b = 8{\cdot}544\ (6)$, $c = 7{\cdot}406\ (4)$ Å, $\alpha = 110{\cdot}51\ (4)$, $\beta = 103{\cdot}49\ (3)$, $\gamma = 94{\cdot}35\ (4)^\circ$, $V = 629{\cdot}2\ (7)$ Å^3, $Z = 2$, $D_m = 1{\cdot}299\ (2)$, $D_x = 1{\cdot}300$ g cm^{-3}, λ(Cu $K\alpha$) = 1·5418 Å, $\mu = 7{\cdot}36$ cm^{-1}, $F(000) = 260$, $T = 288$ K, $R = 0{\cdot}065$ for 1938 reflections. (7) Benzyl 5-methyl-2-oxazolecarbamate, $C_{12}H_{12}N_2O_3$, $M_r = 232{\cdot}24$, $P2_1/c$, $a = 4{\cdot}663\ (6)$, $b = 10{\cdot}48\ (2)$, $c = 23{\cdot}28\ (6)$ Å, $\beta = 90{\cdot}9\ (1)^\circ$, $V = 1137\ (4)$ Å^3, $Z = 4$, $D_m = 1{\cdot}329\ (5)$, $D_x = 1{\cdot}357$ g cm^{-3}, λ(Cu $K\alpha$) = 1·5418 Å, $\mu = 7{\cdot}84$ cm^{-1}, $F(000) = 488$, $T = 288$ K, $R = 0{\cdot}058$ for 1569 reflections. (8) Ethyl 5-phenyl-2-oxazolecarbamate, $C_{12}H_{12}N_2O_3$, $M_r = 232{\cdot}24$, $Pbcn$, $a = 26{\cdot}44\ (1)$, $b = 12{\cdot}206\ (8)$, $c = 7{\cdot}206\ (4)$ Å, $V = 2326\ (2)$ Å^3, $Z = 8$, $D_m = 1{\cdot}321\ (4)$, $D_x = 1{\cdot}327$ g cm^{-3}, λ(Cu $K\alpha$) = 1·5418 Å, $\mu = 7{\cdot}67$ cm^{-1}, $F(000) = 976$, $T = 288$ K, $R = 0{\cdot}050$ for 1650 reflections. (9) Benzyl 4-methyl-2-phenyl-5-oxazolecarbamate, $C_{18}H_{16}N_2O_3$, $M_r = 308{\cdot}34$, $P\bar{1}$, $a = 14{\cdot}99\ (4)$, $b = 9{\cdot}16\ (4)$, $c = 6{\cdot}00\ (2)$ Å, $\alpha = 107{\cdot}8\ (3)$, $\beta = 92{\cdot}6\ (5)$, $\gamma = 96{\cdot}2\ (4)^\circ$, $V = 776\ (5)$ Å^3, $Z = 2$, $D_m = 1{\cdot}319\ (4)$, $D_x = 1{\cdot}319$ g cm^{-3}, λ(Cu $K\alpha$) = 1·5418 Å, $\mu = 7{\cdot}05$ cm^{-1}, $F(000) = 324$, $T = 288$ K, $R = 0{\cdot}065$ for 1605 reflections. (10) Benzyl 2-phenyl-4-oxazolecarbamate, $C_{17}H_{14}N_2O_3$, $M_r = 294{\cdot}32$, $P2_1/a$, $a = 12{\cdot}017\ (2)$, $b = 9{\cdot}745\ (2)$, $c = 13{\cdot}923\ (3)$ Å, $\beta = 113{\cdot}65\ (1)^\circ$, $V = 1493{\cdot}6\ (5)$ Å^3, $Z = 4$, $D_m = 1{\cdot}318\ (6)$, $D_x = 1{\cdot}309$ g cm^{-3}, λ(Cu $K\alpha$) = 1·5418 Å, $\mu = 7{\cdot}10$ cm^{-1}, $F(000) = 616$, $T = 288$ K, $R = 0{\cdot}055$ for 2547 reflections. These related molecules exhibit different inhibitory activities for aldose reductase. In addition to the crystal and molecular structures, the correlation between the molecular conformation and inhibitory activity is reported.

0108-7681/91/050806-08$03.00